Icarus 287 (2017) 175–186

Contents lists available at ScienceDirect

Icarus

journal homepage: www.elsevier.com/locate/icarus

Differentiation and cryovolcanism on Charon: A view before and after New Horizons

S.J. Desch*, M. Neveu

School of Earth and Space Exploration, Arizona State University, Tempe, AZ 85287-1404, USA

ARTICLE INFO

Article history:
Received 21 March 2016
Revised 22 October 2016
Accepted 29 November 2016
Available online 5 December 2016

Keywords:
Charon
Interiors
Satellites
Formation
Volcanism

ABSTRACT

Before the arrival of the *New Horizons* probe at the Pluto-Charon system, we developed a series of models that predicted that Kuiper Belt Objects, even as small and as cold as Charon, have experienced internal ice-rock differentiation and possibly cryovolcanism. Confronting these predictions is a wide array of spectroscopy, imagery, and other data from *New Horizons*. In this article we compare the predictions against the new observations, and find that they largely support the expected history of the Pluto system and the evolution of Charon. Following the collision of two partially differentiated impactors with radii ≈1000 km, a disk of material formed around Pluto, from which Charon and Pluto's other moons formed. Because the impactors did not completely differentiate, the disk contained rocky material from their crusts, explaining the moons' different densities and compositions. Long-lived radionuclides in Charon, assisted by ammonia antifreeze in the ice, melted ice and created a subsurface ocean that eventually refroze ≈1.7 – 2.5 Gyr ago. The freezing of this ocean would have created extensional stresses that possibly created Serenity Chasma, and could have led to widespread resurfacing, explaining the apparently younger age of Vulcan Planum. Buildup of radiogenic heat then created a second, smaller ocean that refroze 0.5–1.7 Gyr ago. As it froze, cryovolcanism would have been enabled, possibly creating Kubrick Mons. Charon's "moated mountains" such as Kubrick Mons have a natural explanation as cryovolcanoes depressing a thin lithosphere over a cryomagma chamber. We offer further predictions about other aspects of Charon's surface. Our previous predictions that Charon is a world shaped by geological activity have been largely borne out by *New Horizons* observations.

1. Introduction

For decades after Charon was discovered (Christy and Harrington, 1978), the strong expectation was that it would be a cold, dead world, perhaps akin to a large comet (Stern, 1989; Simonelli and Reynolds, 1989). The world that *New Horizons* would eventually visit was thought to be ancient, possibly even preserving information about the planetary building blocks of the outer Solar System (McKinnon and Mueller, 1988; Stern, 1989). With a surface temperature ≈55 K (Lellouch et al., 2011) and a pre-encounter radius 606 ± 8 km and density $1720 \pm 150\,\mathrm{kg\,m^{-3}}$ (Gulbis et al., 2006), this body was thought to be too small for cryovolcanism (Schubert et al., 2010), and possibly too small even to differentiate (Stern, 1989; Durand-Manterola, 2003); or, in later studies, too small if differentiated to maintain subsurface liquid in the recent past (Hussmann et al., 2006). Based on these studies, there was no reason to expect geological activity on Charon.

This view began to change in the last decade or so, as observations began to isolate the spectrum of Charon from that of Pluto. These observations revealed the presence of crystalline water ice on Charon's surface (Brown and Calvin, 2000; Buie and Grundy, 2000; Dumas et al., 2001; Cook et al., 2007; Merlin et al., 2010). Crystalline water ice is converted to amorphous form by irradiation from Galactic cosmic rays or even UV photons from the Sun, on relatively short timescales, $\sim 10^7$ year (Cook et al., 2007, and references therein). Crystalline water ice on KBO surfaces was interpreted to mean relative youth and therefore geological activity such as cryovolcanism (Brown and Calvin, 2000; Cook et al., 2007; Famá et al., 2010), as on Quaoar (Jewitt and Luu, 2004). A later theoretical study indicated that the heat of micrometeorite impacts on the surfaces of icy moons was probably sufficient to anneal the surface ice and counteract the amorphizing effects of radiation (Porter et al., 2010). This implies that the presence of crystalline water ice does not necessitate cryovolcanism, despite being suggestive of it.

In addition to crystalline water ice, ammonia hydrates on Charon's surface were detected with increasing certainty by Buie and Grundy (2000), Brown and Calvin (2000), Cook et al. (2007),

* Corresponding author.
E-mail address: steve.desch@asu.edu (S.J. Desch).

http://dx.doi.org/10.1016/j.icarus.2016.11.037
0019-1035/

Merlin et al. (2010), and DeMeo et al. (2015). Since ammonia hydrates also are expected to be destroyed on KBO surfaces by chemical processes initiated by energetic irradiation of roughly 100 eV per molecule, received on KBO surfaces on short (~20 Myr) timescales (Strazzulla and Palumbo, 1998; Cooper et al., 2004), the presence of ammonia hydrates has also been interpreted as requiring some sort of geological activity. As ammonia is a potent antifreeze, ammonia hydrates have been associated with cryovolcanism as that mechanism (Jewitt and Luu, 2004; Cook et al., 2007). It is to be noted, however, that the time to receive ≈100 eV dosages grows quickly with depth, and that ice at only several microns' depth would not receive sufficient irradiation to destroy ammonia hydrates (Fig. 5A of Cooper et al., 2004). Diffusion of NH_3 from the interior into the surface H_2O ice may also create ammonia hydrates (Cruikshank et al., 2015). Therefore, the presence of ammonia hydrates does not necessitate cryovolcanism, although it, too, is suggestive of it. Because of these alternative explanations for crystalline water ice and ammonia hydrates, there was no compelling reason to expect *New Horizons* to find Charon to be a geologically active world.

Motivated by the question of determining whether cryovolcanism is even possible in the past or present on bodies as small as Charon, our research group has built a series of increasingly sophisticated models. Desch et al. (2009) constructed a 1-D (spherically symmetric) model for the thermal internal evolution of KBOs, including the effects of ammonia and partial differentiation. Unlike previous models that assumed fully differentiated bodies (Hussmann et al., 2006), this model assumed KBOs accreted as homogeneous rock-ice mixtures, and that rock and ice within them separated only where and when heating from radioactive decay was sufficient. The predicted structure is a rocky core surrounded by an icy mantle, with liquid possible at the interface, underlying an undifferentiated crust of rock and ice too cold for rock and ice to separate. These undifferentiated rock-ice crusts were a robust prediction of the Desch et al. (2009) model, as was the fact that greater radiogenic heat released in the first 1–2 Gyr of a KBO's history can lead to increased heat flux today and a prolonged duration of subsurface liquid. The model of Desch et al. (2009) assumed that temperatures >176 K, the melting point of ammonia-water mixtures, was needed for rock and ice to separate. In later work, we investigated how these dense rock-ice crusts could overturn with the ice mantle below them via Rayleigh–Taylor instabilities; we determined that layers warmer than 140 ± 15 K would overturn but still would leave undifferentiated crusts tens of km thick on Charon-sized bodies (Rubin et al., 2014). Neveu et al. (2015a) investigated whether the rocky core would crack on small bodies; in most cases it does, allowing hydrothermal circulation through the core, with thermal and geochemical consequences. Neveu et al. (2015b) investigated which dissolved gases might arise in the subsurface ocean and how exolution of such gases might allow liquid to ascend through cracks and enable cryovolcanism. The thermal model was applied to Ceres in particular (Neveu and Desch, 2015) and, in two abstracts, to Haumea (Desch and Neveu, 2015b) and Charon (Desch and Neveu, 2015a). Desch (2015) investigated the state of the two KBOs that collided to form the Pluto-Charon system, demonstrating that their rock-ice crusts would have contributed to the circumplutonian disk from which Charon formed, increasing its density well above that of pure ice. The results of these models are detailed predictions of Charon's origins, composition, internal structure and thermal evolution, and the possibility for cryovolcanism and surface expression.

Other thermal models suggest differentiation and liquid in the Pluto-Charon system. Robuchon & Nimmo (2011) predict full differentiation and the possibility of present-day liquid inside Pluto. Very few thermal evolution models exist for Charon specifically. The models of Hussmann et al. (2006) assumed full separation of rock and ice in Charon, but nevertheless predicted that bodies as small as Charon could retain liquid for several Gyr. Thermal evolution models of Charon were also developed by Malamud and Prialnik (2015). These models also start off with an undifferentiated ice-rock mixture, but the differentiation process is modeled through the multiphase diffusive flow of water through porous rock. The heat of water-rock interaction is also accounted for, but no convective heat transfer occurs, whether in rock as hydrothermal circulation, in liquid, or in ice. The models of Malamud and Prialnik (2015) predict substantial differentiation, but in the absence of convective processes, Charon retains steep temperature gradients and substantial bulk porosity (near 25%) at depths up to 200–300 km. At such depths, temperatures allow water trapped in these poors to be liquid even at the present day.

Now these models and our models are confronted with new data: following its flyby of the Pluto-Charon system in July 2015, the *New Horizons* spacecraft has brought Charon into the realm of geology. Pluto's radius (1187 ± 4 km) and density (1860 ± 13 kg m^{-3} and Charon's radius (606 ± 3 km) and density (1702 ± 20 kg m^{-3}) are now firmly established (Stern et al., 2015), and Charon and Pluto are found to be closer in density and composition than previously expected. Stern et al. (2015) have suggested this may imply that Charon formed as an intact moon from the collision of two undifferentiated impactors. Is the formation of Charon from a circumplutonian disk following a giant impact still consistent with these new compositions?

Imaging of Charon by *New Horizons*' Long-Range Reconnaissance Imager (*LORRI*) and its Multicolor Visible Imaging Camera (*MVIC*) of the *Ralph* instrument package have revealed a world that has been geologically active. A belt of chasmata circles a large fraction (if not all) of the moon, delimiting relatively ancient terrain to the north, and smooth, more sparsely-cratered plains to the south (Stern et al., 2015). The chasmata appear to be extensional features, often with graben features such as Serenity Chasma, consistent with dilation of Charon's ice shell resulting from freezing of a global subsurface ocean, a possibility predicted by Cruikshank et al. (1997) and Moore et al. (2003). From preliminary crater counts and estimates of cratering rates in the Kuiper belt (Schlichting et al., 2013; Greenstreet et al., 2015), the northern ancient terrains appear to be over 4 Gyr old, but Charon's younger equatorial plains (Vulcan Planum; we adopt in this paper the unofficial nomenclature used by the *New Horizons* team) may have been emplaced as early as ≈4 Gyr ago, or as late as 100–300 Myr ago (Stern et al., 2015). Could the chasms and the age dichotomy arise from a global resurfacing event related to the freezing of the subsurface ocean?

Several "moated mountains", including the remarkable Kubrick Mons, have been observed on Charon's limb, in which mountains kilometers high and wide are surrounded by depressions kilometers wide and deep. These mountains resemble the Hawaiian Islands, which are volcanoes depressing the surrounding lithosphere. Could these moated mountains on Charon be cryovolcanically emplaced and depressing their surrounding lithosphere?

Our models make specific predictions addressing each of these questions. In this article we compare our group's model predictions with *New Horizons* data. In Section 2 we use the updated densities of Pluto and Charon and our thermal evolution models for the impactors to argue for formation of Pluto's moons from an impact-generated disk. In Section 3 we discuss the state of Charon immediately after it forms from a disk. In Section 4 we present new calculations of the thermal evolution of Charon that support the existence of liquid water on Charon, at least in the past, and we calculate the timing of freezing of the surface ocean in an attempt to constrain the time of origin of Charon's Vulcan Planum and extensional chasmata, favoring times around 1.7–2.5 Gyr ago. In Section 5, we argue that Kubrick Mons and similar features are

possibly direct evidence for cryovolcanism, perhaps as recently as 0.5–1.7 Gyr ago.

2. Charon's origin from an impact-generated disk

2.1. Background

Since Charon's discovery, the favored hypothesis for the formation of Pluto's largest moon has been origin in a giant impact (McKinnon, 1989; Stern, 1992; Canup, 2005), similar to the origin of the Earth-Moon system (Hartmann and Davis, 1975). Canup (2005) offered two possible scenarios that reproduce the mass ratio and angular momentum of the Pluto-Charon system. The first, the "intact moon" scenario, involves the collision of two undifferentiated bodies with masses typically 70% and 30% of the mass of the Pluto-Charon system; the smaller body remains largely intact throughout the collision but is captured into orbit. In the second, two differentiated bodies of nearly equal mass collide and form a circumplutonian disk; Charon forms from that disk. The formation of a disk is strongly correlated with the differentiation of the bodies, which determines their moments of inertia and therefore the partitioning of angular momentum in the material. Canup (2005) favored the intact moon scenario, in part because it admitted a broader range of input parameters, but primarily because of the composition of the disk. Because the impacting bodies necessarily would have separated rock and ice, their outermost mantles, if fully differentiated, would have been purely water ice; Charon would, if formed from the disk, be pure water ice, inconsistent with its observed density.

The discovery of Nix and Hydra (Weaver et al., 2006) and later Kerberos (Showalter et al., 2011) and Styx (Showalter et al., 2012b), all in nearly circular orbits coplanar with Charon's, and all very nearly in mean motion commensurabilities with Charon, revived the idea of formation from a disk (Stern et al., 2006). Canup (2010) showed that the intact moon scenario could produce a small circumplutonian disk from which Nix and Hydra could form, provided the impactors were rock-ice mixtures surrounded by ice mantles. How the moons ended up being so far from Pluto-Charon, and so close to mean motion resonances with Charon, are outstanding questions. It was early on suggested that they were forced outward by resonant interactions with Charon as it tidally evolved to its present orbit following the giant impact (Ward and Canup, 2006). But this has been called into question, as capture into some of the mean motion resonances is not possible, and the orbits of captured moonlets would be non-circular (Cheng et al., 2014). A promising scenario is one in which disk material is driven outward during Charon's migration, and moonlets form later at a variety of locations, surviving preferentially if near the mean motion resonances (Kenyon and Bromley, 2013; Walsh and Levison, 2015). At any rate, every scenario for Pluto's moons appears to demand formation in a circumplutonian disk.

This left unanswered the question of how Charon could be so dense and contain so much rock along with its ice, since presumably the impactors were differentiated bodies, to form a disk. In response, Desch (2015) showed that in fact the two impactors were unlikely to be completely differentiated, instead retaining crusts of undifferentiated rock and ice several tens of km thick. A very large fraction of the disk arising after the impact actually comes from the undifferentiated crusts of the two bodies, so that the disk contains a significant amount of rock. Desch (2015) showed that if two bodies with densities $\approx 2000\,\mathrm{kg\,m^{-3}}$ and radii 972 km (amounting to 106% of the Pluto-Charon system mass) collided after ≈70 Myr, then they would retain undifferentiated crusts ≈46 km thick. If the outermost 6% of the two bodies escaped the system following the collision, then the innermost 1 Pluto mass would have density $2060\,\mathrm{kg\,m^{-3}}$, and the remaining 1 Charon mass would have density $1630\,\mathrm{kg\,m^{-3}}$, values consistent with the observed densities before the *New Horizons* encounter. Desch (2015) also considered the other moons of Pluto, pointing out that they could sample the bodies' ice mantles (with density $\approx 935\,\mathrm{kg\,m^{-3}}$), their undifferentiated crusts (with density $\approx 2000\,\mathrm{kg\,m^{-3}}$), or any composition in between. Desch (2015) discussed the existing observational evidence and favored scenarios in which the moons had small diameters and high albedos consistent with the mass estimates of Youdin et al. (2012).

Much of this information has been refined since the *New Horizons* encounter. The sizes and albedos of the moons have been determined: Nix has dimensions 54 × 41 × 36 km, and a mean geometric albedo between 0.43 and 0.50, and Hydra has dimensions 43 × 33 km and an albedo ≈0.51; these are such high albedos that these moons must contain cleaner water ice than Charon (Stern et al., 2015). The albedo of Styx was constrained to be $A \approx 0.3\,(D/6\,\mathrm{km})^{-1/2}$ (Showalter et al., 2012a), and with a reported diameter ≈6 km, it must have an albedo similar to Charon's. In contrast, Kerberos appears to be much darker (Showalter and Hamilton, 2015). It is remarkable that Nix, Hydra and Styx appear to be linked in a three-body resonance like the Laplace resonance shared by Io, Europa and Ganymede (Showalter and Hamilton, 2015); in this context Kerberos may have a different origin. On the other hand, Showalter et al. (2012a) constrained the albedo of Kerberos to be $A \approx 0.35\,(D/14\,\mathrm{km})^{-1/2}$, so unless it greatly exceeds a diameter of 14 km, it is probably also Charon-like in composition. Nix, Hydra, and Styx, at any rate, definitely appear to share a common origin, and are mixes of Charon-like material and water ice. The compositional information from *New Horizons* about the moons is consistent with predictions of Desch (2015) for their formation from an impact-generated disk.

As for Charon itself, thanks to *New Horizons*, Pluto's mass, radius, and density have been revised to $1.303 \pm 0.003 \times 10^{22}$ kg, 1187 ± 4 km, and $1860 \pm 13\,\mathrm{kg\,m^{-3}}$, and Charon's mass, radius, and density have been revised to $1.586 \pm 0.015 \times 10^{21}$ kg, 606 ± 3 km, and $1702 \pm 21\,\mathrm{kg\,m^{-3}}$ (Stern et al., 2015). These revised densities, differing by only 10%, are much closer to each other than previous estimates had suggested. While Charon had been estimated to have a density $\approx 1720\,\mathrm{kg\,m^{-3}}$ (Gulbis et al., 2006) or $\approx 1710\,\mathrm{kg\,m^{-3}}$ (Sicardy et al., 2006), other estimates placed its density closer to $1630\,\mathrm{kg\,m^{-3}}$ (Tholen et al., 2008; Desch et al., 2009). Estimates of Pluto's density varied widely, due to the difficulty of distinguishing the planet's limb from its atmosphere during occultations, but a radius 1147 km and a density $2060\,\mathrm{kg\,m^{-3}}$ were often adopted (Tholen et al., 2008; Desch et al., 2009). The closeness in densities led (Stern et al., 2015) to suggest that the impactors that formed the Pluto-Charon system were undifferentiated or only "modestly differentiated" at the time of the impact, with implications for when the impact took place and how quickly bodies accreted in the Kuiper Belt. The revision in densities calls into question whether a disk with the right composition to form Pluto and Charon could arise from the impact of two partially differentiated bodies (in which rock and ice have fully separated except for a ≈50 km thick undifferentiated rock-ice crust), as hypothesized by Desch (2015). Below we investigate whether this scenario is consistent with the revised data.

2.2. Revised calculations

We essentially repeat the calculations of Desch (2015), modeling the thermal evolution and crustal thickness of two identical progenitor impactors. Naturally the two impactors could be of different size, but for the sake of simplicity we assume two identical progenitors. Exploration of different size ratios, or other parameters affecting thermal evolution of the progenitors, would be beyond the scope of this paper and unnecessary for our purpose,

Table 1
Initial conditions for thermal evolution simulations of Charon and its progenitors.

Parameter	Units	Progenitor	Charon
Radius	km	994	606
Density	kg m^{-3}	1840	1702
Degree of rock hydration		0%	100%
Rock density	kg m^{-3}	3250	2900
Rock fraction in fines	kg kg^{-1}	0–0.75	0–0.75
Ammonia content w.r.t. H_2O	kg kg^{-1}	1%	1%
Surface temperature	K	40	40
Initial uniform temperature	K	40	60 or 100
Simulation start time	Myr after CAIs	4–7	100 or 500
Simulation end time	Gyr	0.1	4.56

which is merely to show that Charon's density is consistent with its formation from a disk. Instead of varying their possible radii and densities, we fix their radii to be 994 km. The Kuiper Belt very likely contains several bodies larger than 1000 km in radius today (Trujillo et al., 2001), and would have contained many more early in solar system history (Stern, 1991). We also fix their densities to be 1840 kg m^{-3}. If the densities of rock and ice are 3250 kg m^{-3} and 935 kg m^{-3}, respectively, then the mass fraction of each impactor that is rock is $f_r = 0.691$. Large KBOs typically have densities of this order. We go beyond the work of Desch (2015) by assuming the progenitors may have formed early enough to accrete live ^{26}Al. If the progenitors formed a time Δt after calcium-rich, aluminum-rich inclusions (CAIs), the fraction of aluminum in them that was radioactive is $^{26}Al/^{27}Al = 5 \times 10^{-5} \exp(-\Delta t/\tau)$, where $\tau = 1.03$ Myr. We calculate the powerful radiogenic heating from ^{26}Al decay following Castillo-Rogez et al. (2007). We consider different values of Δt in a range from about 3–7 Myr. We consider the accretion timescale to range from 10^5 to 10^6 years (Weidenschilling, 2004). Such timescales are slow enough that heat of accretion can be radiated away (see Desch, 2015). We also go beyond (Desch, 2015) by assuming, in analogy with the makeup of chondrites and in line with previous studies (Bland et al., 2013; Travis et al., 2015; Neveu and Desch, 2015), that the rocky component of the progenitors is distributed between micron-sized fines and millimeter-sized chondrule-like particles. Fines are likely to remain suspended in liquid or ice, and will not separate, which is consistent with the suggestion of Stern et al. (2015) that the progenitors were incompletely differentiated. We vary x_f, the fraction of rocky mass that is in micron-sized fines, between 0 and 0.75. We consider all of these effects when calculating the internal structure and thermal evolution of the impactors.

We evolve progenitor KBOs using the 1-D spherically symmetric code described in detail by Desch et al. (2009). This code performs time-dependent calculations of the internal temperature profile and structure of bodies made of rock and ice. It is applicable to non-tidally heated objects roughly 300–1500 km in radius, as it neglects porosity (significant below this radius range) and the compressibility of rocky and icy materials (significant above this range) as well as high-pressure phases of ice. The original code was subsequently modified by Neveu et al. (2015a) to include a detailed model of the effects core fracturing, hydrothermal circulation, and rock hydration and dehydration. Neveu and Desch (2015) added in the ability to model incomplete differentiation due to suspension of fine-grained rock in the ocean and ice shell.

Inputs to the code are body radius, bulk density, densities of dry and hydrated rock end members, ammonia and fine-grained rock content, initial degree of rock hydration, surface temperature, initial temperature (isothermal radial profile), time of formation, and total simulation time. These inputs are detailed in Table 1. From the density inputs, a bulk rock:ice ratio is determined. The initial structure is assumed homogenous. Mass is distributed assuming spherical symmetry on a fixed-volume 1-D grid, with a specified number of zones evenly distributed in radius (200 in this study). Material densities are assumed constant with depth; Neveu et al. (2015a) showed that neglecting compressibility resulted in radii overestimates of only ~10 km and pressure underestimates that do not exceed 15% for a Ceres-like object, when compared to structures computed with pressure-dependent equations of state for materials. Calculating the effects of compression for a fully differentiated Charon progenitor, we also find that the assumption of incompressibility underestimates central pressures by only a few percent.

The internal energy in each grid zone is computed from the initial temperature using equations of state, detailed by Desch et al. (2009), for rock (independently of its degree of hydration) and ice (which includes water ice I, liquid water, liquid ammonia, and ammonia dihydrate I). For this study, ice is assumed to contain 1% ammonia by mass, initially in the form of ammonia dihydrate. For the Pluto-Charon progenitors, it is assumed that any accretional heating has been dissipated before the starting time of the simulation. From this initial state, the internal energy E_i in each grid zone i of outer radius r_i is updated after a time step Δt. This time step (fixed at 50 years in this study) satisfies a Courant condition $\Delta t < \min[(\Delta r)^2/(2\kappa_d)]$, where κ_d is the thermal diffusivity. Energy changes are due to heat fluxes F_i out of each zone, as well as net heating rates due to radioactive decay ($Q_{i,\,rad}$), gravitational energy changes due to changes in internal structure ($Q_{i,\,grav}$), and chemical hydration and dehydration reactions ($Q_{i,\,hydr}$):

$$\frac{E_i(t+\Delta t) - E_i(t)}{\Delta t} = 4\pi r_{i-1}^2 F_{i-1} - 4\pi r_i^2 F_i + Q_{i,\mathrm{rad}}(t) + Q_{i,\mathrm{grav}} + Q_{i,\mathrm{hydr}} \quad (1)$$

Heat fluxes, assumed conductive, are computed using a finite-difference scheme as:

$$F_i = -\frac{k_i + k_{i+1}}{2} \frac{T_{i+1} - T_i}{(r_{i+1} - r_{i-1})/2} \quad (2)$$

Here, k_i are the thermal conductivities in each grid zone; chosen expressions are given by Desch et al. (2009) and Neveu et al. (2015a). T_i are the temperatures, computed such that E_i is the energy required to raise the mix of rock and ices from 0 K to T_i, including phase transitions, using the equations of state mentioned above. Rocky fines have lower thermal conductivity (k_i = 1–4.2 W m^{-1} K^{-1}) than ice ($567/T \approx$2–14 W m^{-1} K^{-1}), making the mantle more insulating according to the formalism of Desch et al. (2009). They also increase its viscosity by a factor $(1 - \phi/\phi_m)^{-2}$, where ϕ is the volume fraction of rock fines in ice and $\phi_m \approx 0.63$ is a critical volume fraction (Mueller et al., 2009). The boundary conditions are zero heat flux at the center (by symmetry), and a fixed surface temperature T_{surf}. T_{surf} is usually equated to the effective temperature resulting from the balance of insolation and radiated energy, under the assumption that insolation dominates surface heat fluxes:

$$T_{surf} = \left(\frac{L_\odot\ (1-A)}{16\pi\ a_\odot^2\ \sigma} \right)^{1/4} \quad (3)$$

where $L_\odot$ is the solar luminosity, A is the Bond albedo, and σ is the Stefan–Boltzmann constant. For Charon and its progenitors, we adopt T_{surf} = 40 K.

Heat transfer by convection (advection and diffusion), rather than solely by conduction, can occur in three settings. In the ice layer, solid-state convection is assumed to occur if the Rayleigh number Ra, computed at the midpoint of the layer, exceeds a critical value Ra_c. Following (Desch et al., 2009), the heat flux through grid zones undergoing convection is then computed as $k_i \times (Ra/Ra_c)^{0.25} \times (\Delta T/\Delta r)$. Vigorous convective heat transfer is also assumed to occur in any grid zone containing more than 2% ice

melt ("slush", or ocean if the layer is fully melted). We capture this by setting the thermal conductivity to an arbitrary value of 400 W m^{-1} K^{-1}, high enough to obtain a near-isothermal temperature profile across the slush layer, but low enough to satisfy the Courant criterion. The third setting is hydrothermal circulation in the core; again the convective heat flux is parameterized in terms of the conductive heat flux and Rayleigh number, this time computed for fluid flow in a porous medium (Neveu et al., 2015a). Hydrothermal circulation occurs in core layers that satisfy three conditions: (1) these layers must be porous, either due to initial porosity or fracturing in brittle rock by thermal expansion mismatch at grain boundaries, thermal pressurization of fluid-filled pores, and/or rock volume changes due to changes in its degree of hydration; (2) there must be sufficient liquid water to circulate: fractured rock layers must directly underlie a volume of fluid that exceeds the total pore volume in these layers; (3) the Rayleigh number across these layers must exceed a critical value.

The heating rate $Q_{i,\,\mathrm{rad}}(t)$ due to the decay of radionuclides j is given by

$$Q_{i,\mathrm{rad}}(t) = M_{rock,i} \sum_j N_j \ \Delta E_j \ \ln(2)/t_{1/2,j} \ \exp(-\ln(2)/t_{1/2,j} \ \times \ t), \tag{4}$$

where $M_{rock,\,i}$ is the mass of silicate rock in a zone i, N_j is the number of atoms of the nuclide j per kg of rock, ΔE_j is the energy produced per decay, and $t_{1/2,\,j}$ is the nuclide half-life. These parameters are given by Desch et al. (2009) for the long-lived radionuclides ^{40}K, ^{232}Th, ^{235}U, and ^{238}U, and by Neveu et al. (2015a) for the short-lived radionuclide ^{26}Al. CI abundances are assumed (Lodders, 2003).

Ice-rock differentiation occurs if the temperature in a zone exceeds a threshold T_{diff}. It is assumed that differentiation is initiated by ice melting at a temperature of first melt (solidus) that depends on initial ammonia content. For non-negligible amounts of ammonia (arbitrary mass fraction of 10^{-2} in ice), we set T_{diff} = 176 K, the H_2O–NH_3 eutectic; otherwise we set T_{diff} = 273 K. In practice, melting first occurs in the central zones and differentiation proceeds outward. In all the zones exceeding T_{diff}, the code redistributes mass by first filling the innermost zones with rock, then the zones surrounding this rocky chondrule core with mixed liquids, ammonia dihydrate (ADH), and rock fines, and finally the outermost differentiated zones with mixed water ice and rock fines (Neveu and Desch, 2015). This approach ensures mass conservation. Volume changes are precluded by choosing fixed densities for liquid water and ammonia, slightly different from their actual values: the density of liquid water $\rho_{\mathrm{H2O(l)}}$ is equated to that of ice $\rho_{\mathrm{H2O(s)}}$, and the density of ammonia $\rho_{\mathrm{NH3(l)}}$ is determined by mass balance: $\rho_{\mathrm{NH3(l)}}{}^{-1} = \rho_{\mathrm{H2O(l)}}{}^{-1} + (\rho_{\mathrm{H2O(s)}}{}^{-1} + \rho_{\mathrm{ADH(s)}}{}^{-1})/X_c$, where $\rho_{\mathrm{ADH(s)}}{}^{-1}$ is the density of ammonia dihydrate, and $X_c = 0.321$ is the eutectic ammonia mass fraction. Densities were provided by Desch et al. (2009).

Differentiation leads to a gravitationally unstable configuration, with an ice mantle underneath a denser, undifferentiated crust. Such a configuration is prone to Rayleigh–Taylor instabilities, which Rubin et al. (2014) showed act on geological timescales in zones where $T_i > T_{\mathrm{diff}} \approx 140$ K. This value of T_{diff} is adopted in the late stages of differentiation, once it has proceeded out to more than half the radius of the body.

Differentiation generates heat due to gravitational energy release. The gravitational potential energy U_g is calculated at each time step:

$$U_g = -G \int_0^{r_p} 4\pi r^2 \rho(r) \frac{M(r)}{r} dr \tag{5}$$

where $M(r)$ is the mass enclosed within a sphere of radius r, r_p is the body's radius, and G is the gravitational constant. If differentiation has redistributed mass and changed U_g during a time step, this energy difference ΔU_g is redeposited uniformly throughout all differentiated grid zones, out to a radius R_{diff}. The corresponding heating rate $Q_{i,\,\mathrm{grav}}$ in Eq. (1) is given by:

$$Q_{i,\mathrm{grav}} = \Delta U_g \frac{r_i^3 - r_{i-1}^3}{R_{\mathrm{diff}}^3} \tag{6}$$

Upon rock hydration or dehydration, heat is produced or consumed, respectively. The heat released by serpentinization reactions, H_{hydr}, ranges between −450 and −700 kJ (kg dry rock)$^{-1}$ and is arbitrarily set at the midrange value, −575 kJ kg^{-1} (Neveu et al., 2015a). The net heating rate $Q_{i,\,\mathrm{hydr}}$ is calculated in each grid zone with rock mass $M_{i,\,\mathrm{rock}}$ as

$$Q_{i,\mathrm{hydr}} = \Delta X_{i,\mathrm{hydr}} \times M_{i,\mathrm{rock}} \times (-H_{\mathrm{hydr}})/\Delta t. \tag{7}$$

Here, $\Delta X_{i,\,\mathrm{hydr}}$ is the variation in $X_{i,\,\mathrm{hydr}}$, the degree of hydration in each zone i, after a time step. $X_{i,\,\mathrm{hydr}}$ is 0 if the silicates in this zone are completely dehydrated and 1 if they are fully hydrated. For dehydrating silicates, $X_{i,\,\mathrm{hydr}}$ decreases linearly with temperature between 700 K and 850 K (Neveu et al., 2015a). $X_{i,\,\mathrm{hydr}}$ is allowed to increase in a given layer only if (1) the temperature of this layer is below 850 K and decreasing, (2) this layer is undergoing hydrothermal circulation, and (3) there is enough liquid to hydrate this layer. Upon hydration and dehydration, masses and volumes of rock and water are adjusted to conserve total mass and volume, such that the rock densities vary linearly between 3250 kg m^{-3} and 2900 kg m^{-3} for dry and hydrated rock, respectively. These values, adopted for this study, are inputs to the code and can be modified by the user.

In Fig. 1 we display the results of six simulations, in which we assume Δt = 7, 5 or 4 Myr, and the fraction of solids in micron-sized fines is either $x_f = 0$ or $x_f = 0.58$. These figures display the internal temperature as different colors, as a function of position in the body on the vertical axis (with the center at $r = 0$ at the bottom, and the surface at r = 994 km, on top) and time after formation on the horizontal axis, from 0 to 100 Myr. In all cases, the amount of live ^{26}Al at time of formation has a strong bearing on the extent of differentiation (rock-ice separation) and when it occurs. Considering first the cases without fines, for Δt = 4 Myr,

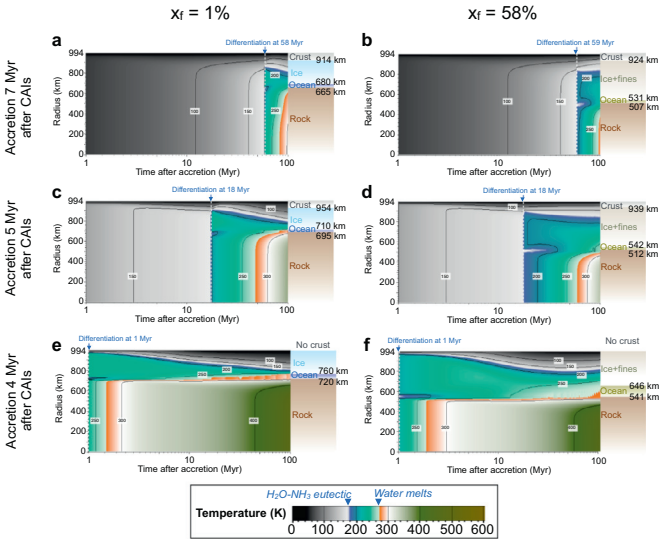

Fig. 1. Thermal evolution of the two Pluto-Charon progenitors. Temperature as a function of radius within the bodies and as a function of time after formation is plotted as a color (legend at bottom). We consider two different fines fractions, $x_f = 1$ and $x_f = 0.58$, and times of formation after CAIs of Δt = 7, 5 or 4 Myr. At the right of each panel is the compositional structure of each body after 100 Myr of evolution.

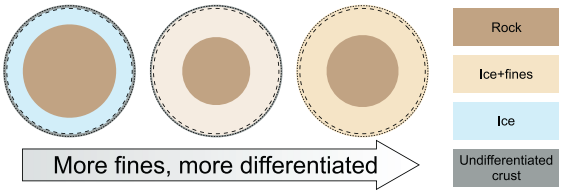

Fig. 2. Possible internal structures (drawn to scale) of the two progenitors (each with radius 994 km and density 1840 kg m^{-3}) that yield Pluto and Charon with their observed densities. Pluto forms from the cores and icy mantles of each body; Charon forms from material between the dashed and dotted curves; material outside the dotted curve escapes. From left to right the fraction of rocky material in micron-sized fines increases from $x_f = 0\%$ to 75%. Higher fines fractions require thinner crusts to match Charon's density.

differentiation occurs in $<$ 1 Myr and is complete, leaving essentially no crust (Fig. 1e). If $\Delta t = 5$ Myr, differentiation starts at 18 Myr and leaves behind a crust with thickness 40 km (Fig. 1c). For $\Delta t \geq 7$ Myr, heating by ^{26}Al is negligible, differentiation takes place after about 60 Myr, and leaves behind a crust 80 km thick (Fig. 1a). The rock fraction in fines has no bearing on the timing of differentiation, but the extent of differentiation (crustal thickness) differs slightly in the case with fines comprising 58% of the rocky material. For Δt =4, 5, and 7 Myr, respectively, differentiation leaves essentially no crust (Fig. 1f), a thicker crust with thickness 60 km (Fig. 1d), or a slightly thicker crust 75 km thick (Fig. 1b). The thickness of the crust essentially measures where the temperature never exceeded 140 K, the approximate temperature needed to allow Rayleigh–Taylor instabilities to overturn the dense rock-ice crust with the less dense ice mantle below it.

The crusts in the no-fines case are slightly thicker than those found by Desch (2015) for similar bodies, demonstrating the sensitivity of crustal thickness to the transport of heat out of the core to its thermal conductivity, here assumed higher (4.2 W K^{-1} m^{-1}; Table 1) than by Desch (2015). It also demonstrates that many combinations of the many input parameters such as ^{26}Al content, fines fraction, and surface temperature can lead to the same crustal thickness. This degeneracy is depicted in Fig. 2, which displays a family of solutions with different fines fractions x_f (and times of formation Δt) that reproduce the bulk compositions of Pluto and Charon.

The masses and bulk densities of Pluto and Charon are reproduced if the bodies collide as follows. The combined mass of the two impactors is 103.6% of the Pluto-Charon system, so we assume that the outermost 3.5% of each impactor's mass is ejected from the system during the impact. This outermost material, from the uppermost 11.6 km of each body, is composed of undifferentiated rock and ice with the mean composition of the two bodies. An escape fraction of 3.5% is very plausible: Canup (2005) found escape fractions of 0–8% in simulations that formed a disk. Pluto will form from the innermost 86.1% of the mass, comprising the rocky core and some of the ice (or ice plus fines) mantle from each impactor, out to a radius of 942.1 km in each body. The disk and Charon will form from the intermediate 10.5% of the mass, from material between 942.1 km and 982.4 km. In this scenario, if x_f is the fraction of rocky material that is in fines that remain well mixed with ice, then the volume fraction of fines plus ice that is fines is $\phi = (1 + 1.5580/x_f)^{-1}$, and the density of the fines plus ice mixture is $\rho_{fi} = \rho_i + \phi(\rho_r - \rho_i)$. We note that the main effects of redistributing some of the rocky component into fines suspended in the ice mantle are: the thermal conductivity of the ice mantle is somewhat lowered; the ice mantle is thickened and the core size reduced; and radiaoctive elements are put nearer the surface. The net result of these competing effects is to slightly decrease the internal temperatures. To reproduce Pluto and Charon, the progenitors must be differentiated out to the radius

$$R_{diff} = \left(\frac{\rho_{PL} - \rho_{fi}}{2(\bar{\rho} - \rho_{fi})}\right)^{1/3} R_{PL}, \quad (8)$$

where $\rho_{PL} = 1860$ kg m^{-3} and $R_{PL} = 1187$ km are the density and radius of Pluto, and $\bar{\rho} = 1840$ kg m^{-3} is the presumed bulk density of the progenitors.

This equation is derived by making three assumptions: the progenitors start at density $\bar{\rho}$ and differentiate out to R_{diff}, so $\rho_{rock}R^3_{core,prog} + \rho_{fi}\left(R^3_{diff} - R^3_{core,prog}\right) = \bar{\rho}R^3_{diff}$; Pluto is fully differentiated, so that $\rho_{rock}R^3_{core,PL} + \rho_{fi}\left(R^3_{PL} - R^3_{core,PL}\right) = \rho_{PL}R^3_{PL}$; and Pluto's core mass is the sum of the two progenitors' core masses so that $\rho_{rock}R^3_{core,PL} = 2\rho_{rock}R^3_{core,prog}$. The crustal thickness of each progenitor must be $\Delta R = 994$ km $- R_{diff}$. For $x_f = 0$ (no fines), to reproduce Pluto and Charon we must have $R_{diff} = 949.0$ km and $\Delta R =$ 45.0 km, very close to what Desch (2015) found. For $x_f = 0.58$, one needs $R_{diff} = 964.0$ km and $\Delta R = 30.0$ km, and for $x_f = 0.75$, one needs $R_{diff} = 981.6$ km and $\Delta R = 12.4$ km. Fines fractions x_f $>$0.75 do not reproduce Pluto and Charon (at least for our presumed progenitor density and size). From our thermal evolution models, we find a fines fraction $x_f = 0$ leads to crustal thickness $\Delta R = 45$ km if $\Delta t \approx$5 Myr after CAIs (Fig. 1c). A fines fraction $x_f = 0.58$ leads to crustal thickness $\Delta R = 30$ km for accretion at somewhat shorter times 4 Myr $< \Delta t <$ 5 Myr (interpolating between Fig. 1d and f). These values of R_{diff} are unlikely to change after 100 Myr. We therefore conclude that plausible parameters do indeed allow Charon to form from a disk and have its observed density.

To summarize, we consider the impact of two progenitors with radii 994 km and bulk densities 1840 kg m^{-3}. In the most workable scenarios, they form at $\Delta t \approx$5 Myr after CAIs, to retain some live ^{26}Al that helps them differentiate and reduce their crustal thickness. During the collision, for these parameters, 3.5% of the mass must escape, a very plausible fraction. The cores and part of the icy mantles of each body form Pluto, and a fraction of each progenitor's mass, from the outermost crust and icy mantle of each body, contributes to a circumplutonian disk from which Charon and the other moons form. The bulk composition of Pluto is reproduced, and the bulk composition of the disk matches Charon's, if the crustal thickness is about 45 km (for no fines) or 30 km ($x_f = 0.58$), or 12 km ($x_f = 0.75$). No particular value of x_f in the range 0–0.75 seems preferred (although fine fractions higher than $\approx$0.6 may yield crusts too thin to withstand impacts for tens of Myr), but reproducing the crustal thicknesses apparently requires $\Delta t \approx$5 Myr. Regardless of fines content, differentiation starts about 18 Myr later, or 23 Myr after CAIs. As long as the impact occurs after this time, Charon can form from a circumplutonian disk.

This timing is consistent with the impact occuring during the orbital chaos ensuing as Neptune migrated outward, which in the Nice model (Tsiganis et al., 2005), is timed to coincide with the Late Heavy Bombardment of the inner solar system around 650 Myr after the birth of the solar system. But the impact need not occur so late: if the Late Heavy Bombardment can be attributed to another cause, e.g., destabilization of the orbits of planets interior to Mercury (Volk and Gladman, 2015), then Neptune's migration and the orbital chaos it causes in the outer solar system could have occurred much earlier. An impact in the first 100 Myr is very reasonable (Kenyon and Bromley, 2013). At this earlier time, more KBOs would have been present (Stern, 1991) and the low relative velocities favored by impact models would have been more likely (McKinnon, 1989; Canup, 2005). We consider especially plausible a scenario in which Neptune starts to migrate at around 30–100 Myr, scatters one impactor into the other, and then catches the newly formed Pluto-Charon system in a sweeping resonance. Notably, Charon and Pluto's moons would not be lost to

gravitational perturbations as Pluto migrated outward with Neptune. (Pires et al., 2015).

One outcome we consider unlikely is one in which the impact occurred before the bodies started to differentiate. Perfectly homogeneous bodies would not give rise to Pluto and Charon having different bulk densities. In addition, an impact between two undifferentiated bodies would probably not result in formation of a disk (Canup, 2005), without which the orbits of Pluto's other moons are difficult to explain. Finally, the fact that Nix and Hydra have compositions more ice-rich than Charon strongly suggests contributions from the icy mantles of partially differentiated impactors.

3. Initial assembly of Charon in the disk

Many features of the Pluto-Charon system are consistent with formation from a circumplutonian disk. Accretion from a disk is very likely to lead to observable differences in its surface reflectance spectrum. It is presumed that most KBOs form slowly enough (timescales $\sim 10^5$ years or longer) that the gravitational potential energy released during their accretion can be radiated away. Forming from a disk, Charon must have accreted much more rapidly than that: following the giant impact with the Earth, the Moon probably formed in less than $\sim 10^2$ years, or 10^5–10^6 orbits (Salmon and Canup, 2012). Presumably Charon formed in a similar number of orbits, or about 10^4 years. These timescales are too short for Charon to radiate away its energy, and it is a simple matter (Desch, 2015) to show that as each shell with radius r accretes onto Charon, it attains a temperature

$$T(r) = \bar{T}\left[1 + \mathcal{A}\left(\frac{r}{R}\right)^2\right]^{1/2}, \tag{9}$$

where $\mathcal{A} = 8\pi G\bar{\rho}R^2/(3C_{P,0}\bar{T})$, $\bar{\rho} = 1702\,\mathrm{kg\,m^{-3}}$ being Charon's average density and $R = 606$ km its radius, and $\bar{T}$ being the initial average temperature of the disk material from which Charon forms. If the impact occurs at ≈0.5 Gyr, $\bar{T} \approx 100$ K is an appropriate average (Desch, 2015), but if the impact occurs at ≈0.1 Gyr after solar system formation, before the bodies have heated up due to long-lived radioactive decay, we estimate $\bar{T} \approx 60$ K. Here it is assumed that the temperature-dependent heat capacity is $C_P(T) = C_{P,0}(T/T_0)$, where $C_{P,0} = 461\,\mathrm{J\,kg^{-1}\,K^{-1}}$ and $T_0 = 100$ K are appropriate for a Charon-like mixture of rock and ice. We therefore calculate that if the impact occurred at 0.5 Gyr, then temperatures would exceed 176 K (the temperature of first melt for a water-ammonia mixture) for $r > 319$ km, or 85% of Charon's mass, allowing a few percent of the ice to melt into a eutectic mixture of ammonia and water; temperatures at the surface would exceed 273 K, and we estimate that 5% of even pure water ice could melt. If the impact occurred at 0.1 Gyr, surface temperatures would reach 221 K, and temperatures would exceed 176 K for $r > 470$ km, representing 53% of Charon's mass.

This material would remain melted for considerable time. A warm layer (ΔR) ~ tens of km thick will stay warm for a time $\sim (\Delta R)^2/\kappa$ before its heat is conducted to the surface and radiated away. Here $\kappa = k/(\rho C_P)$, which we estimate as $\kappa \sim 4 \times 10^{-6}\,\mathrm{m^2\,s^{-1}}$ for typical parameters. Heat will be conducted to the surface from depths of 10 km in ~1 Myr, and even at only 10 m depth, liquid may take a year to cool. It seems inevitable that if Charon formed from a disk, then a substantial fraction of its mass near the surface was at least partially melted, for long enough for rocky material to react with liquid.

As discussed in Section 2, we assume Charon formed from a homogeneous mixture of disk material from the outer parts of the two impactors, deriving partially from their icy mantles and partially from their undifferentiated crusts of rock and ice. In the crusts we assume a mix of micron-sized fines and millimeter-sized "chondrules", and the ice mantles may also contain fines. In contrast to the conclusion of Desch (2015), we do *not* expect any these particles to settle through Charon's surface layers, as only < 10% of it is liquid. The standard equation for the Stokes settling time for particles of density $\rho_r \approx 3250\,\mathrm{kg\,m^{-3}}$ and diameter D to slide a distance ΔR through Charon's outer layers with density $\rho_c \approx 1700\,\mathrm{kg\,m^{-3}}$, due to Charon's gravity $g = 0.28\,\mathrm{m\,s^{-2}}$, is

$$t_{\mathrm{settle}} = \frac{18(\Delta R)\eta}{(\rho_r - \rho_c)\,g\,D^2}, \tag{10}$$

Despite there being some melt, the volume fraction of the surrounding material is dominated by water ice with viscosity $\eta > 10^{14}$ Pa s. Thus, assuming the rocky material is in particles millimeter-sized or smaller, settling even 10 m through the rock-ice outer layers of Charon would take >100 Myr. Because silicate particles are exposed to liquid but will not settle out of the layers, they should be aqueously altered in place, even as closely as tens of meters from the surface. Impact gardening would mix this subsurface ice and aqueously altered rock onto the surface.

Our prediction of partial melt of ice in a rock/ice crust may explain a curious result obtained by several groups fiting Charon's spectrum. Many analyses have supported the presence of a dark absorber on Charon's surface that has no prominent spectral features, and which is spectrally neutral in the visible but absorbing with bluish slope in the near-infrared (Buie and Grundy, 2000; Cook et al., 2007; Protopapa et al., 2008; Cruikshank et al., 2015). Buie and Grundy (2000) derive the "dark neutral absorber" from spectra of Charon, but compare it to various materials, including two sulfates and two phyllosilicates—montmorillonite [$(Na, Ca)_{0.33}(Al, Mg)_2Si_4O_{10}(OH_2 \cdot nH_2O]$ and kaolinite [$Al_2Si_2O_5(OH)_4$]. On Earth, these common clays are produced by the weathering of aluminosilicate minerals such as feldspars, usually in hot, moist climates. As pointed out by Buie and Grundy (2000), the bluish slope to the neutral absorber seems to argue for OH in the structure of the substance, as in phyllosilicates. Kaolinite appears to provide a slightly better fit to Charon's spectrum than anything else (Buie and Grundy, 2000; Cook et al., 2007; Merlin et al., 2010). Merlin et al. (2010) model the dark absorber on Charon as a mix of this blue component and amorphous carbon. Whatever the exact composition, this component appears to make up a volume fraction ϕ ≈30% (Merlin et al., 2010), 10%–30% (Cook et al., 2007), or possibly 40% (Protopapa et al., 2008) of Charon's surface. It can certainly be the case that other minerals may explain the neutral, bluish absorption, but of all the minerals tried so far, phyllosilicates like kaolinite provide the best fit. This is a surprise, because phyllosilicates are the result of rock reacting with liquid water. Liquid water on Charon's surface is not generally expected, but is a natural outcome if Charon formed from a disk. We suggest that Charon's crust may even hold ammoniated phyllosilicates like those observed on Ceres (de Sanctis, 2015).

Considering how Charon should form from a circumplutonian disk, we envision the following scenario. Following the impact, a mix of rock and ice from the progenitors' ice mantles and crust is homogeneously mixed in the disk, and Charon forms from that mix. To match Charon's bulk density, rock (with density $\rho_r = 3250\,\mathrm{kg\,m^{-3}}$) must have a mass fraction 0.633 and volume fraction ϕ ≈33% in the disk and Charon, including its outer layers. Because several percent of ice was melted, there was opportunity for silicate rock to react with liquid and be aqueously altered into clay-like minerals. Assuming the rocky component consumes 13% of its mass in ice, and swells to minerals with density $\approx 2900\,\mathrm{kg\,m^{-3}}$ (Desch and Neveu, 2015b), the volume fraction of the aqeuously altered solid material would be ϕ ≈45%. These volume fractions are consistent with those derived from spectroscopy, providing evidence that rock and ice did not separate in Charon's surface layers. This material would be a mix of millimeter-sized chondrules and

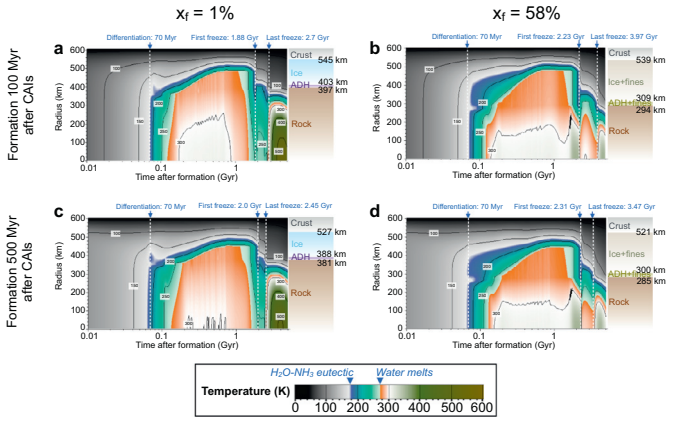

Fig. 3. Thermal evolution of Charon. Temperature as a function of radius within Charon and as a function of time is plotted as a color (legend at bottom), as in Fig. 1. The impact that generated the disk from which Charon formed is considered to occur at 0.1 Gyr (top panels) or 0.5 Gyr (bottom panels) after CAIs. Two fines fractions are considered: $x_f = 0.01$ (left panels) and $x_f = 0.58$ (right panels). In all cases Charon partially differentiates after 70 Myr of evolution, leaving crusts 61–85 km thick. Charon generally starts to freeze after about 2 Gyr of evolution, melts again, then freezes again for the last time after about 3 Gyr of evolution, leaving a mantle of water and ammonia dihydrate (ADH) ices above a rocky core and below an undifferentiated rock/ice crust.

micron-sized fines; the proportions matter little to the reflectance spectrum. Considering this initial structure for Charon, we now consider its internal thermal evolution.

4. Thermal evolution of Charon

We calculate the thermal evolution of Charon after the impact using the same thermal evolution code described in Section 2. We assume an initial composition of ice and rock, as described in Section 3. We consider the fraction of rocky material in micron-sized fines to vary in the range $0 < x_f < 0.75$. Input parameters for progenitor and Charon calculations are shown in Table 1. The surface temperature is set at 40 K, corresponding to radiative equilibrium for a body at 39 AU with albedo 0.37. As discussed in Section 3, the outer layers of Charon are likely to accrete warm, and stay warm for many Myr, even producing melt on its surface. But Charon's outer layers are very unlikely to differentiate as a result, because the liquid content is too low to allow Stokes flow and rock-ice separation, and does not extend very deep below the surface. Rayleigh–Taylor instabilities potentially could operate at temperatures as low as 140 K, but they rely on the interior having already separated into a rocky core and icy mantle, so that the crust is denser than the layers below it. This is unlikely to occur on Charon. Thermal evolution will lead to differentiation of its interior only after about 70 Myr, by which time the heat in the uppermost 100 km of Charon will have diffused to the surface. Differentiation from the inside out will occur on Charon, but it will not be aided by initially high surface temperatures. We assume that differentiation will create a rocky core comprised of chondrules, but that fines may remain suspended in the liquid.

The subsequent evolution of Charon is shown in Fig. 3, which shows the temperature as a function of radius within Charon, and time after its formation, for four combinations of parameters: $x_f =$ 0.01 or 0.58, and a time of the impact either 0.1 Gyr or 0.5 Gyr after solar system formation.

These times bracket the range we consider plausible: we favor cases where the impact occurs after the progenitors have started to differentiate, some 70 Myr after solar system formation; but Charon must form long enough ago to yield surfaces with crater ages >4 Gyr (Stern et al., 2015). For an impact at 0.1 Gyr, the initial temperature is set at 60 K (but more long-lived radionuclides are retained), while if the impact occurs at 0.5 Gyr, the initial temperature is set at 100 K. Surface temperatures in either case are set at 40 K. In all cases, temperatures inside are sufficient to initiate rock-ice separation, and a rocky core surrounded by a mantle of ice (or ice with fines) forms rapidly at about 70 Myr after the impact. A subsurface ocean of liquid between the core and the mantle first appears in this stage.

Differentiation is always partial, and the original rock/ice is left behind in a crust of thickness 61 – 85 km in these runs. Liquid persists for a long time. While it is present, heat transport is convective, cooling the interior rapidly; the near-surface frozen layers remain conductive. Radiogenic heating decreases over time, and at about 2 Gyr after the Charon-forming impact, liquid in the subsurface ocean freezes. This limits the ability of heat to be transported out of the core, and Charon's interior heats up and the ice actually remelts. This liquid eventually refreezes at about 2.5 Gyr after the impact for the case with no fines, and at about 3.5–4.0 Gyr after the impact for the case with $x_f = 0.58$.

Charon's thermal evolution depends somewhat strongly on what fraction of rock is in fines that remain suspended in the ice, and less strongly on the time of the impact. For the case with essentially no fines ($x_f = 0.01$), the time of last freezing occurs at 2.8 Gyr after CAIs if the impact occurs at 0.1 Gyr, or 3.0 Gyr after CAIs if the impact occurs at 0.5 Gyr. A later time of impact means Charon has less heating from long-lived radionuclides, but it also means the progenitors were warmed more before the impact. A later time of impact leads to somewhat thicker crusts ($\approx 79 - 85$ km instead of $\approx 61 - 67$ km), but the total energy and the time of final melting are hardly different. Fines in the ice mantle, on the other hand, affect the crustal thickness slightly and greatly affect the time of final freezing. For the case with $x_f = 0.58$, the time of last freezing occurs at about 4.0 Gyr whether the impact occurs at 0.1 or 0.5 Gyr. This is attributable to a decrease in thermal conductivity in the ice-fines mantles: we assume hydrated fines have conductivity $1\,W\,m^{-1}\,K^{-1}$, whereas ice in the outer portions of the ice mantle has a higher thermal conductivity. The decrease in thermal conductivity leads to only slightly thicker crusts ($\approx 67 - 85$ km instead of $\approx 61 - 79$ km), but the time of freezing is extended by over 1 Gyr.

For the range of impact times and fine fractions we have considered, liquid is present from soon (70 Myr) after the impact, and a subsurface ocean persists for many Gyr. It first freezes between 2.0 and 2.8 Gyr after CAIs (2.5–1.7 Gyr ago), is remelted, and finally freezes anywhere from 2.8 to 4.0 Gyr after CAIs, i.e., from about 1.7 to 0.5 Gyr ago. We note that these behaviors could not have been predicted by previous models. Hussmann et al. (2006) assumed complete separation of rock and ice, and circulation of water through the core, so that the ocean could only monotonically cool and freeze. Malamud and Prialnik (2015) considered liquid to only exist within a porous rock matrix, and an ocean is not predicted.

The first large-scale global freezing of subsurface liquid at about 1.7–2.5 Gyr should lead to substantial volume changes ΔV in the ocean, because of the difference between the densities of liquid water ($\rho_w \approx 1000$ kg m^{-3}) and ice Ih ($\rho_w \approx 935$ kg m^{-3}; Croft et al. (1988)). Ice is about 7% larger in volume than liquid, and this is true even if the liquid contains substantial ammonia (Cook et al., 2007). [If the ocean contains fines that cannot settle, the volume fraction will be somewhat less: for $x_f = 0.58$, the volume fraction of rock in the ocean is $\phi = 0.271$, and the ocean will expand by about 5% in volume.] The maximum mass of liquid in our simulations is typically 2.4×10^{20} kg. This ocean freezes rather rapidly in tens of Myr. During this geologically short interval, $\approx 2.4 \times 10^{17}$ m^3 of liquid freezes, expanding in volume by about $\Delta V \approx 1.7$

$\times$ 10^{16} m^3. This volume increase could lead to several geologically observable consequences.

Freezing of a subsurface ocean would be conducive to forming fractures in the ice mantle, and could lead to outpourings of liquid (cryolava) on the surface. As just ≈10% of a liquid reservoir freezes, it compresses the liquid, overpressurizing it by the ~50 MPa needed for it to ascend ~500 km (Fagents, 2003; Manga and Wang, 2007; Neveu and Desch, 2015; O'Brien et al., 2015). Freezing of the first subsurface ocean could lead to enough liquid extruding onto the surface of Charon to cover its southern hemisphere to a depth of about 7 km, easily resurfacing it. If the widespread resurfacing of Vulcan Planum was due to effusive cryovolcanism triggered by the freezing of a subsurface ocean, our modeling strongly suggests that it took place only 1.7–2.5 Gyr ago.

Freezing of the first subsurface ocean could also lead to extensional stresses and faulting of the surface as observed by *New Horizons*. The volume increase associated with freezing of the subsurface ocean would expand Charon's global circumference by about 23 km, comparable to the width of Serenity Chasma at its widest, ≈60 km (Stern et al., 2015). The timing of this extension is again most likely during the time of the first large-scale freezing event, at about 1.7–2.5 Gyr ago.

After the subsurface ocean freezes, radiogenic heat buildup in the core can partially melt it again, creating liquid that again circulates through the core and cools it. The mass of this second, colder ocean is limited by the amount of ammonia antifreeze available, and is typically ≈10^{19} kg,only a few percent of the volume of the first ocean. Being such much lower in volume, we do not expect this second freezing to result in extensive tectonics, and global resurfacing would be limited to only < 0.3 km, but freezing of a eutectic ocean could pressurize liquid and drive cryovolcanism, as described next.

5. Cryovolcanism and Kubrick Mons

Potentially strong evidence for cryovolcanism on Charon comes from the "moated mountains" of Kubrick Mons and similar features observed by *New Horizons* on Charon's limb. Kubrick Mons appears to be a large, almost conical mountain, surrounded by a deep moat that is depressed relative to the landscape around it (Stern et al., 2015). Situated near the terminator at the time of the *New Horizons* flyby, the mountain casts a long shadow into the moat region. The base of the mountain is partially in shadow, while part of the moat region behind it appears extra bright. These features are not conclusive but are suggestive of a slightly raised lip or rim around the moat. We estimate the base of the conical mountain to have radius 17 km, and its height to be 3–4 km. The moat appears to be circular, with a depth of perhaps 2 km, and a distance to the edge of the depression (or the raised rim) about 30 km, although its location near the terminator makes it difficult to exactly ascertain its geometry. The most direct interpretation of the morphology appears to be that there is a conical mountain sitting in a large, circular depression, with a slightly raised rim around it.

A simple interpretation of this object might be an impact crater with an especially large central peak. This interpretation is unsatisfactory in view of the truly large size of the central peak relative to the "crater", and the rarity of this morphology: obvious impact craters in the same field of view have much steeper crater rims. We instead interpret this as a large mountain, probably emplaced cryovolcanically, that has depressed the lithosphere surrounding it by isostatic adjustment (Fig. 4). An appropriate Earth analog may be the volcanically emplaced Hawaiian Islands, which have also depressed the lithosphere around them. The Hawaii Trough is a depression in the sea floor extending in a near-circular arc around the islands of Maui and Hawaii, with a radius of about 130 km. Within it the depth of the ocean floor is about 5600 m, compared

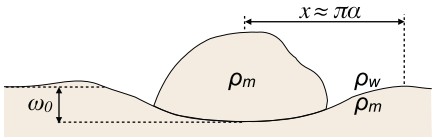

Fig. 4. Geometric parameters for calculations of the lithospheric deformation surrounding Kubrick Mons.

to an average seafloor depth of about 5000 m around the Hawaiian Islands. In fact, the ocean floor is probably more than 600 m deeper in the trough, as it has been infilled by sediments (Moore et al., 1994). Extending even further around the islands, with a radius near 250–300 km, is the Hawaii arch, a slight elevation of 200 m above the surrounding seafloor (Walcott, 1970).

To determine whether a cryovolcano on Charon would cause a depression in the lithosphere with the right depth and radius to match observations, we use the equations of Turcotte and Schubert (1982) for a linear load on an unbroken lithosphere; Lambeck and Nakiboglu (1980) describe crustal deformation for a circular disk sitting on top of the crust. In either geometry, the key input is the flexural rigidity D, given by

$$D = \frac{E\,h^3}{12\,(1-\nu^2)}, \tag{11}$$

where E is the Young's modulus, ν is Poisson's ratio (we arbitrarily assume $\nu = 1/4$, a common value, for all materials), and h is the effective crustal thickness. A key quantity is the flexural parameter α, where

$$\alpha = \left[\frac{4D}{(\rho_m - \rho_w)\,g}\right]^{1/4}, \tag{12}$$

and ρ_m is the density of the mantle material and ρ_w is the density of seawater. If the line load (force per length) is V_0, the maximum deflection of the crust will be at the line ($x = 0$), and will be $w(0) = V_0\alpha^3/(8D)$. The deflection at a distance x from the line will be

$$w(x) = w_0\, e^{-x/\alpha}\left(\cos\frac{x}{\alpha} + \sin\frac{x}{\alpha}\right). \tag{13}$$

The distance to the maximum elevation (forebulge) is then $\approx\pi\alpha$, and the elevation there will be $-0.0432\,w_0$. Substitution of typical values yields results that reasonably match the Hawaiian Islands. Assuming $\rho_m = 3300\,kg\,m^{-3}$, $\rho_w = 1000\,kg\,m^{-3}$, $g = 9.8\,m\,s^{-2}$ and $E = 70$ GPa, and assuming a lithospheric thickness $h = 34$ km yields $D = 2.4 \times 10^{23}$ N m and $\alpha = 81$ km. For the Hawaiian Islands, the maximum deflection is about 10 km, implying a load $V_0 = 3.6 \times 10^{13}\,N\,m^{-1}$. For these parameters, the forebulge should lie at a distance 255 km from the center, and have a maximum elevation of 430 m. For the case of axisymmetric loads from conical mountatins, the coefficients differ, but the dependencies on physical quantities are similar (Lambeck and Nakiboglu, 1980).

Applying this model to Charon amounts to determining whether reasonable parameters for material properties and lithospheric thickness yield the observed flexure parameters. To avoid uncertainties due to the geometry, we compare directly to the Hawaiian Islands. The ratio of flexure parameters on Charon and Earth will be

$$\frac{\alpha_C}{\alpha_E} = \left(\frac{D_C}{D_E}\right)^{1/4}\left(\frac{g_C}{g_E}\right)^{-1/4}\left[\frac{(\rho_m-\rho_w)_C}{(\rho_m-\rho_w)_E}\right]^{-1/4}. \tag{14}$$

We set $\alpha_C/\alpha_E = (30\,km)/(250\,km)$ (the ratio of their forebulge distances), $g_C/g_E = (0.28\,m\,s^{-2})/(9.8\,m\,s^{-2})$, $(\rho_m - \rho_w) = 900\,kg\,m^{-3}$ for Charon, and $(\rho_m - \rho_w) = 2300\,kg\,m^{-3}$ for Earth. From this we determine that $D_C = 2.3 \times 10^{-6}\,D_E$. Given Charon's low gravity, its crust must have deformed more readily than Earth's. From there it

is simple to estimate the lithospheric thickness of Charon's crust:

$$\left(\frac{D_C}{D_E}\right) = \left(\frac{E_C}{E_E}\right)\left(\frac{h_C}{h_E}\right)^3 \quad (15)$$

Assuming $E = 0.5$ GPa for ice (Lorenz and Shandera, 2001), we find $h_C = 0.069\, h_E$, or about 2.3 km. We can estimate other quantities using numerical values. If the forebulge around Kubrick Mons lies at 30 km, then $\alpha \approx 9.6$ km. We estimate $D_C = 5.5 \times 10^{17}$ N m. If we estimate the line load as $V_0 = Mg/(2R)$, where $R = 17$ km is the radius of the mountain, $H \approx 4$ km its height, and $M = \rho_m \pi R^2 H/3 \approx 1.1 \times 10^{15}$ kg, we find $V_0 \approx 9 \times 10^9$ N m^{-1}. Combining these, we estimate $w_0 = 1.8$ km, very consistent with the imagery of Kubrick Mons. The height of the forebulge at 30 km would then be about 80 m.

A cryovolcanically emplaced mountain depressing the surrounding lithosphere is consistent with the observations, provided the lithospheric thickness—the depth to the brittle-ductile transition—is only 2.3 km. This is remarkably thin. Imagining the mountain exists for ~1 Myr (see below), this transition point will occur where the strain rate can exceed $\dot{\epsilon} > (1\,\mathrm{Myr})^{-1}$ due to the stress σ induced by the mountain. We estimate σ to be of the order of the pressure underneath the mountain, $P \sim Mg/(\pi R^2) \approx 0.3$ MPa. The underlying crust will flow on Myr timescales in response to this stress where the viscosity equals the critical viscosity $\eta_{crit} = \sigma/(2\dot{\epsilon}) = 5 \times 10^{18}$ Pa s. From the figures presented by Rubin et al. (2014), this requires temperatures of about 155 K for pure ice, and will not differ substantially if the ice contains ammonia or impurities. For the lithospheric thickness to be only 2.3 km, the depth at which temperatures >155 K are reached must lie only 2.3 km deep. This is considerably closer to the surface than models of Charon's overall internal temperature would suggest; these temperatures are not typically found within 55 km of the surface. Moreover, the heat flux from the base of the lithosphere to the surface must be profoundly greater. The results suggest a temperature gradient ~ 40 K km^{-1}, an order of magnitude greater than expected. These features suggest that the lithosphere is normally thicker and not so easily deformed, and that the cryovolcano depressed the lithosphere during a transiently warm state.

In the context of our hypothesis that Kubrick Mons is an emplaced cryovolcano, we attribute the remarkably thin lithosphere to the existence of a cryomagma chamber or pluton at shallow depths below the cryovolcano. If a spherical pluton ≈15 km in radius were created and filled with a eutectic ammonia-water mixture at 176 K, rising to roughly 2.5 km below the surface at temperature ≈50 K, it could easily express itself as a feature very much like Kubrick Mons. Such a feature would necessarily be transient, however. Assuming an average thermal conductivity of ice ≈ 6 W m^{-1} K^{-1}, the heat flux would have been about 300 mW m^{-2}, or a total energy loss across the base of Kubrick Mons of about 0.25 GW. The latent heat of fusion of the liquid stored in the pluton, ~4×10^{21} J, would be lost in just about 0.5 Myr as the pluton froze. As the pluton froze, the volume increase could have caused about 7% of the liquid to be extruded onto the surface, a volume equal to that of Kubrick Mons. The rate of emplacement would have been remarkable, ~ 70 kg s^{-1}, but not unreasonable. For comparison, over the past few centuries lava has been outpouring from Mauna Loa at a rate of about 3000 kg s^{-1} (Lipman, 1995). Finally, we note that the parameters discussed above are similar to those obtained by Giese et al. (2008) in their models of the deformation of Enceladus' lithosphere. They derived heat fluxes on the order of 250 mW m^{-2}, a flexure parameter $\alpha = 3.14$ km, an effective lithosphere thickness $h = 0.3$ km, and a brittle-ductile layer transition depth around 2.1 km.

How likely is it that cryovolcanism could have occurred on Charon? We view it as very likely: at any point in time when subsurface liquid existed, ascent to the surface could have occurred by a number of mechanisms. At any time subsurface liquid existed, if the liquid held fines, fines might settle out in liquid chambers where the vigor of convective currents is insufficient to resuspend fines. Being less dense than its surroundings, the resulting liquid could then ascend buoyantly in cracks opened by freezing pressurization stresses, or through simple diapirism. The ascent may be halted by freezing, or by neutral buoyancy near the surface where porosity could decrease the near-surface material density below the density of liquid water-ammonia mixtures. This situation would lead to the emplacement of cryomagma chambers that would progressively cool into plutonic intrusions. With or without fines, liquid could also ascend buoyantly due to exsolution of gases in it, depending on the geochemistry of the ocean, as described by Neveu et al. (2015b). These mechanisms might act at any time liquid is present. In addition, during the last stages of liquid presence, pressurization of liquid in freezing pockets could have forced liquid upward into near-surface plutons.

Assuming Kubrick Mons and the other moated mountains are emplaced cryovolcanoes, when were they created? Given our prediction that subsurface liquid last froze about 0.5 to 1.7 Gyr ago, we view it as unlikely that these would be currently active cryovolcanoes. Should they be currently active, the large heat flux ~ 300 mW m^{-2} would raise the surface temperature by about 10 K locally, leaving a recognizable infrared signature. Instead, we interpret moated mountains as indicative of a *past* episode of cryovolcanism, when there was substantial subsurface liquid. Additionally, noting that Kubrick Mons and other putative cryovolcanoes sit on Vulcan Planum and must have been emplaced *after* the resurfacing of Charon's southern hemisphere, we regard fluid pressurization during freezing of liquid as the most likely ascent mechanism, and the most likely time of formation to be when the subsurface liquid last froze, about 0.5–1.7 Gyr ago.

6. Conclusions

In this article we have pulled together the various predictions our group has made about the Pluto-Charon system and especially Charon, to test these predictions against the new data from *New Horizons*, and to build a coherent scenario for Charon's origin and evolution.

We argue that Charon probably formed from a circumplutonian disk created during a giant impact. The strong consensus is that Pluto's smaller moons formed from a disk, to explain their coplanarity and proximity to mean motion commensurabilities. Whether Charon formed from a disk has been contested, Canup (2005) favoring the intact moon hypothesis because of the perception that Charon would be low-density ice, and Canup (2010) favoring Charon forming as an intact moon and the other moons forming from a small circumplutonian disk. Likewise, Stern et al. (2015) noted the similarity of Pluto and Charon in density and argued that the impactors were undifferentiated or "modestly differentiated". When such bodies collide, they tend to form Charon as an intact moon, not a disk (Canup, 2005). In contrast, Desch (2015) argued, and we argue here using updated data, that Charon did form from a disk, and it ended up with its observed density because the disk contained material not just from an icy mantle, but from the undifferentiated rock-ice crusts of the progenitors as well. The ice may contain fines, but a family of solutions with different fines fractions x_f (the fraction of rocky material in micron-sized fines) in the range 0–0.75 yield a circumplutonian disk and Charon with its observed density. The solutions invoke two identical progenitors ≈994 km in radius and with bulk density 1840 kg m^{-3}, that form $\Delta t \approx 5$ Myr after CAIs to contain some live ^{26}Al. (Although we did not explore these possibilities, presumably a wide range of progenitor masses, etc., could also yield similar re-

sults.) This scenario naturally leads to Pluto and Charon with their observed masses and densities, and is consistent with the observation that the other moons Nix, Hydra, Styx (and possibly Kerberos) are a mix of Charon-like and icier material. For formation of $\Delta t \approx 5$ Myr after CAIs, the progenitors are differentiated by 18 Myr later, or 23 Myr after CAIs, and we favor a collision soon after that, 30–100 Myr in solar system evolution.

We argue that Charon should accrete rapidly from the disk. Following the Moon-forming impact, standard models predict formation of the Moon within a few $\times 10^2$ years, or roughly $10^5 - 10^6$ orbits. If Charon formed in a similar fashion, it would not have taken more than $\sim 10^4$ years to form. As Desch (2015) discussed, this is too fast for the heat of accretion to be radiated during accretion, and therefore its outer layers should be partially melted. If the impact occurs at 0.1 Gyr, the average temperature of the disk material is close to 60 K, and due to the inclusion of 1% ammonia leads to a few percent of the ice melting on Charon's surface. If the impact occurs later, at 0.5 Gyr, the average temperature of the disk material is closer to 100 K, and temperatures on Charon's surface are sufficient to melt 5–10% of the ice. During this initial stage, despite the presence of liquid, particles are unlikely to settle, nor is the crust to overturn. On timescales that depend on the depth, the liquid will refreeze. The surface materials will remain in place in an undifferentiated crust even as Charon (partially) differentiates inside. During the time some liquid exists, we anticipate aqueous alteration of the rocky materials, perhaps producing phyllosilicates on Charon's surface. The conditions of aqueous alteration are likely to include low temperature (0°C to −100°C) alteration by an ammonia-rich (ammonia mass fraction probably $X \approx 0.1 - 0.3$) liquid, with relatively low water-to-rock ratio ($W/R < 0.2$). We plan further investigations to predict the mineralogy of such aqueous alteration products, but note that phyllosilicates generally are consistent with the bluish slope inferred from Charon's near-infrared reflectance spectrum (Buie and Grundy, 2000).

We have calculated the thermal evolution of Charon. The thickness of its crust and the time of final freezing of the subsurface ocean depend on time of the impact that formed Charon, and the fraction of rock material that is fines. For the range of parameters we considered (time of impact at 0.1 Gyr or 0.5 Gyr, fines fractions $x_f = 0.01$ or $x_f = 0.58$), Charon internally differentiates within 70 Myr of the impact, but only partially, leaving behind a crust of original material 61–85 km thick. Liquid is present in a subsurface ocean from the time of formation, reaching at greatest extent 2.4×10^{20} kg (about 20% of the mass of Earth's oceans), and persists for about 2 Gyr before freezing at about 1.7–2.5 Gyr ago. The freezing is geologically rapid (< 0.1 Gyr) and can lead to considerable expansion and pressurization of the liquid. Effusive cryovolcanism during this first freezing stage possibly could have resurfaced Charon's southern hemisphere and Vulcan Planum to several km depth. The expansion of the ocean also could have increased Charon's circumference by >20 km, leading to extensional stresses and possibly explaining surface features such as Serenity Chasma. We note that preliminary crater counts and estimates of cratering rates in the Kuiper belt (Schlichting et al., 2013; Greenstreet et al., 2015) yield ages of >4 Gyr for Charon's northern ancient terrains, and the younger equatorial plains such as Vulcan Planum appear to be as old as 4 Gyr or perhaps as young as 100–300 Myr ago (Stern et al., 2015). The age difference between the two regions is therefore highly uncertain—as much as 4 Gyr or as little as a fraction of a Gyr—but it is significant that there is an age difference. We predict an age difference of about 2–3 Gyr.

Following this, radiogenic heat buildup in the core can melt a smaller amount of liquid, aided by ammonia antifreeze. As this second, eutectic, ocean freezes, pressurization of liquid could drive liquid to the surface, expressed as cryovolcanoes. We interpret Kubrick Mons and other moated mountains as cryovolcanoes emplaced from a transient magma chamber only a few kilometers below the surface. The weight of the cryovolcano depressed the surrounding lithosphere, in analogy with the Hawaiian Islands. Kubrick Mons and the other putative cryovolcanoes were probably formed during the last freezing of the eutectic ocean, about 0.5–1.7 Gyr ago. Kubrick Mons and the other moated mountains are indeed situated on, and are younger than, Vulcan Planum.

In this paper we have applied to the Pluto/Charon system the models our research team has developed over the last decade to understand the thermal evolution of Kuiper belt objects (Desch et al., 2009; Rubin et al., 2014; Desch, 2015; Neveu and Desch, 2015; Neveu et al., 2015a, 2015b). These models predict that Kuiper belt objects should experience partial differentiation, including: rocky cores and icy mantles, overlaid by undifferntiated rock-ice crusts; prolonged persistence of subsurface liquid; and possibly cryovolcanism. Some aspects of Pluto and Charon would appear to be supportive of cryovolcanism, but can be attributed to other causes: crystalline water ice and ammonia dihydrates may have alternative sources that do not require current replenishment of the surface, and the possible existence of phyllosilicates on Charon's surface may be attributable to aqueous alteration soon after Charon's formation from a disk. Other aspects of Pluto and Charon, though, do suggest partial differentiation and cryovolcanism. Charon's bulk density and the orbits and compositions of Pluto's other moons argue for formation from a circumplutonian disk, generated by the impact of two partially differentiated progenitors. The evidence for extensional stresses in Serenity Chasma attributable to freezing of subsurface liquid, the resurfacing of Charon's southern hemisphere, especially Vulcan Planum, and the existence of moated mountains like Kubrick Mons, argue for one-time existence of subsurface liquid and cryovolcanism on Charon.

Acknowledgments

This work was supported by NASA Earth and Space Science Fellowship grant PLANET14F-0032 and by NASA Outer Planets Research grant NNX14AR25G (PI S. Desch). The thermal evolution code used in this paper is freely available at https://github.com/MarcNeveu/IcyDwarf.

References

Bland, P.A., Travis, B.J., Dyl, K.A., Schubert, G., 2013. Giant convecting mudballs of the early solar system. In: Lunar and Planetary Science Conference, Vol. 44, p. 1447.
Brown, M.E., Calvin, W.M., 2000. Evidence for crystalline water and ammonia ices on Pluto's satellite Charon. Science 287 (5450), 107–109.
Buie, M.W., Grundy, W.M., 2000. The distribution and physical state of H_2O on charon. Icarus 148 (2), 324–339.
Canup, R.M., 2005. A giant impact origin of Pluto-Charon. Science 307 (5709), 546–550.
Canup, R.M., 2010. On a giant impact origin of charon, nix, and hydra. Astron. J. 141 (2), 35.
Castillo-Rogez, J.C., Matson, D.L., Sotin, C., Johnson, T.V., Lunine, J.I., Thomas, P.C., 2007. Iapetus' geophysics: rotation rate, shape, and equatorial ridge. Icarus 190, 179–202.
Cheng, W.H., Lee, M.H., Peale, S.J., 2014. Complete tidal evolution of Pluto–Charon. Icarus 233, 242–258.
Christy, J.W., Harrington, R.S., 1978. The satellite of Pluto. Astron. J. 83, 1005.
Cook, J.C., Desch, S.J., Roush, T.L., Trujillo, C.A., Geballe, T.R., 2007. Near-infrared spectroscopy of Charon: possible evidence for cryovolcanism on Kuiper belt objects. Astrophys. J. 663 (2), 1406.
Cooper, J.F., Christian, E.R., Richardson, J.D., Wang, C., 2004. Proton irradiation of Centaur, Kuiper Belt, and Oort Cloud objects at plasma to cosmic ray energy. In: The First Decadal Review of the Edgeworth-Kuiper Belt, pp. 261–277. Springer.
Croft, S.K., Lunine, J.I., Kargel, J., 1988. Equation of state of ammonia-water liquid: derivation and planetological applications. Icarus 73 (2), 279–293.
Cruikshank, D.P., Grundy, W.M., DeMeo, F.E., Buie, M.W., Binzel, R.P., Jennings, D.E., Olkin, C.B., Parker, J.W., Reuter, D.C., Spencer, J.R., Stern, S.A., Young, L.A., Weaver, H.A., 2015. The surface compositions of Pluto and Charon. Icarus 246, 82–92.
Cruikshank, D.P., Roush, T.L., Moore, J.M., Sykes, M.V., Owen, T.C., Bartholomew, M.J., Brown, R.H., Tryka, K.A., 1997. The surfaces of Pluto and Charon. In: Pluto and Charon, Vol. 1. University of Arizona Press Tucson, pp. 221–268.

DeMeo, F.E., Dumas, C., Cook, J.C., Carry, B., Merlin, F., Verbiscer, A.J., Binzel, R.P., 2015. Spectral variability of Charon's 2.21-μm feature. Icarus 246, 213–219.
Desch, S., Neveu, M., 2015a. Charon quandaries. In: AAS/Division for Planetary Sciences Meeting Abstracts, Vol. 47, pp. 210–228.
Desch, S.J., 2015. Density of Charon formed from a disk generated by the impact of partially differentiated bodies. Icarus 246, 37–47.
Desch, S.J., Cook, J.C., Doggett, T., Porter, S.B., 2009. Thermal evolution of Kuiper belt objects, with implications for cryovolcanism. Icarus 202 (2), 694–714.
Desch, S.J., Neveu, M., 2015b. On the origin of Haumea. In: Lunar and Planetary Science Conference, Vol. 46, p. 2082.
Dumas, C., Terrile, R.J., Brown, R.H., Schneider, G., Smith, B.A., 2001. Hubble space telescope NICMOS spectroscopy of Charon's leading and trailing hemispheres. Astron. J. 121 (2), 1163.
Durand-Manterola, H.J., 2003. Internal structure of planetary icy bodies. In: EGS-AGU-EUG Joint Assembly, Vol. 1, p. 7389.
Fagents, S.A., 2003. Considerations for effusive cryovolcanism on Europa: the post–Galileo perspective. J. Geophys. Res. 108 (E12), 5139.
Famá, M., Loeffler, M.J., Raut, U., Baragiola, R.A., 2010. Radiation-induced amorphization of crystalline ice. Icarus 207 (1), 314–319.
Giese, B., Wagner, R., Hussmann, H., Neukum, G., Perry, J., Helfenstein, P., Thomas, P.C., 2008. Enceladus: an estimate of heat flux and lithospheric thickness from flexurally supported topography. Geophys. Res. Lett. 35 (24).
Greenstreet, S., Gladman, B., McKinnon, W.B., 2015. Impact and cratering rates onto Pluto. Icarus 258, 267–288.
Gulbis, A.A.S., Elliot, J.L., Person, M.J., Adams, E.R., Babcock, B.A., Emilio, M., Gangestad, J.W., Kern, S.D., Kramer, E.A., Osip, D.J., Pasachoff, D.M., Souza, S.P., Tuvikene, T., 2006. Charon's radius and atmospheric constraints from observations of a stellar occultation. Nature 439 (7072), 48–51.
Hartmann, W.K., Davis, D.R., 1975. Satellite-sized planetesimals and lunar origin. Icarus 24 (4), 504–515.
Hussmann, H., Sohl, F., Spohn, T., 2006. Subsurface oceans and deep interiors of medium-sized outer planet satellites and large trans-neptunian objects. Icarus 185 (1), 258–273.
Jewitt, D.C., Luu, J., 2004. Crystalline water ice on the Kuiper belt object (50000) Quaoar. Nature 432 (7018), 731–733.
Kenyon, S.J., Bromley, B.C., 2013. The formation of Pluto's low-mass satellites. Astron. J. 147 (1), 8.
Lambeck, K., Nakiboglu, S.M., 1980. Seamount loading and stress in the ocean lithosphere. J. Geophys. Res. 85 (B11), 6403–6418. (1978–2012).
Lellouch, E., Stansberry, J., Emery, J., Grundy, W., Cruikshank, D.P., 2011. Thermal properties of Pluto's and Charon's surfaces from Spitzer observations. Icarus 214 (2), 701–716.
Lipman, P.W., 1995. Declining growth of mauna loa during the last 100,000 years: Rates of lava accumulation vs. gravitational subsidence. In: Mauna Loa Revealed: Structure, Composition, History, and Hazards. Wiley Online Library, pp. 45–80.
Lodders, K., 2003. Solar system abundances and condensation temperatures of the elements. Astrophys. J. 591 (2), 1220–1247.
Lorenz, R.D., Shandera, S.E., 2001. Physical properties of ammonia-rich ice: application to titan. Geophys Res Lett 28 (2), 215–218.
Malamud, U., Prialnik, D., 2015. Modeling Kuiper belt objects Charon, Orcus and Salacia by means of a new equation of state for porous icy bodies. Icarus 246, 21–36.
Manga, M., Wang, C.-Y., 2007. Pressurized oceans and the eruption of liquid water on europa and enceladus. Geophys Res Lett 34 (7), L07202.
McKinnon, W.B., 1989. On the origin of the Pluto-Charon binary. Astrophys. J. 344, L41–L44.
McKinnon, W.B., Mueller, S., 1988. Pluto's structure and composition suggest origin in the solar, not a planetary, nebula. Nature 335, 240–243.
Merlin, F., Barucci, M.A., De Bergh, C., DeMeo, F.E., Alvarez-Candal, A., Dumas, C., Cruikshank, D.P., 2010. Chemical and physical properties of the variegated Pluto and Charon surfaces. Icarus 210 (2), 930–943.
Moore, J.G., Normark, W.R., Holcomb, R.T., 1994. Giant hawaiian landslides. Annu. Rev. Earth Planet Sci. 22, 119–144.
Moore, J.M., Schenk, P.M., Pappalardo, R.T., McKinnon, W.B., 2003. The "geology" of Pluto and Charon. In: EGS - AGU - EUG Joint Assembly, p. 7936.
Mueller, S., Llewellin, E.W., Mader, H.M., 2009. The rheology of suspensions of solid particles. In: Proceedings of the Royal Society of London A, rspa20090445, p. 28.
Neveu, M., Desch, S.J., 2015. Geochemistry, thermal evolution, and cryovolcanism on Ceres with a muddy ice mantle. Geophys. Res. Lett. 42 (23).
Neveu, M., Desch, S.J., Castillo-Rogez, J.C., 2015a. Core cracking and hydrothermal circulation can profoundly affect Ceres' geophysical evolution. J. Geophys. Res. 120 (2), 123–154.
Neveu, M., Desch, S.J., Shock, E.L., Glein, C.R., 2015b. Prerequisites for explosive cryovolcanism on dwarf planet-class Kuiper belt objects. Icarus 246, 48–64.
O'Brien, D.P., Travis, B.J., Feldman, W.C., Sykes, M.V., Schenk, P.M., Marchi, S.T.R.C., Raymond, C.A., 2015. The potential for volcanism on Ceres due to crustal thickening and pressurization of a subsurface ocean. In: Lunar and Planetary Science Conference, Vol. 46, p. 2831.
Pires, P., Winter, S.M.G., Gomes, R.S., 2015. The evolution of a Pluto-like system during the migration of the ice giants. Icarus 246, 330–338.
Porter, S.B., Desch, S.J., Cook, J.C., 2010. Micrometeorite impact annealing of ice in the outer Solar System. Icarus 208 (1), 492–498.
Protopapa, S., Boehnhardt, H., Herbst, T., Cruikshank, D., Grundy, W., Merlin, F., Olkin, C., 2008. Surface characterization of Pluto and Charon by L and M band spectra. Astron. Astrophys. 490 (1), 365–375.
Rubin, M.E., Desch, S.J., Neveu, M., 2014. The effect of Rayleigh–Taylor instabilities on the thickness of undifferentiated crust on Kuiper Belt Objects. Icarus 236, 122–135.
Robuchon, G., Nimmo, F., 2011. Thermal evolution of Pluto and implications for surface tectonics and a subsurface ocean. Icarus 216, 426–439.
Salmon, J., Canup, R.M., 2012. Lunar accretion from a roche-interior fluid disk. Astrophys. J. 760, 83.
de Sanctis, M.C., et al., 2015. Ammoniated phyllosilicates with a likely outer solar system origin on (1) ceres. Nature 528, 241–244.
Schlichting, H.E., Fuentes, C.I., Trilling, D.E., 2013. Initial planetesimal sizes and the size distribution of small Kuiper Belt Objects. Astron. J. 146 (2), 36.
Schubert, G., Hussmann, H., Lainey, V., Matson, D., McKinnon, W., Sohl, F., Sotin, C., Tobie, G., Turrini, D., Van Hoolst, T., 2010. Evolution of icy satellites. Space Sci Rev 153 (1–4), 447–484.
Showalter, M.R., Hamilton, D.P., 2015. Resonant interactions and chaotic rotation of Pluto's small moons. Nature 522 (7554), 45–49.
Showalter, M.R., Hamilton, D.P., Stern, S.A., Weaver, H.A., Steffl, A.J., Young, L.A., 2011. New satellite of (134340) Pluto: S/2011 (134340) 1. Int. Astron. Union Circ. 9221, 1.
Showalter, M.R., Weaver, H.A., Stern, A., Steffl, A.J., Hamilton, D.P., Buie, M.W., Merline, W.J., Young, L.A., Mutchler, M., Soummer, R., Throop, H.B., 2012a. Pluto's P4 and P5: latest results for Pluto's tiniest moons. In: AAS/Division for Planetary Sciences Meeting Abstracts, pp. 304–307.
Showalter, M.R., Weaver, H.A., Stern, S.A., Steffl, A.J., Buie, M.W., Merline, W.J., Mutchler, M.J., Soummer, R., Throop, H.B., 2012b. New satellite of (134340) Pluto: S/2012 (134340) 1. Int. Astron. Union Circ. 9253 (1).
Sicardy, B., Bellucci, A., Gendron, E., Lacombe, F., Lacour, S., Lecacheux, J., Lellouch, E., Renner, S., Pau, S., Roques, F., Widemann, T., Colas, F., Vachier, F., Vieira Martins, R., Ageorges, N., Hainaut, O., Marco, O., Beisker, W., Hummel, E., Feinstein, C., Levato, H., Maury, A., Frappa, E., Gaillard, B., LavayssiÅre, M., Di Sora, M., Mallia, F., Masi, G., Behrend, R., Carrier, F., Mousis, O., Rousselot, P., Alvarez-Candal, A., Lazzaro, D., Veiga, C., Andrei, A.H., Assafin, M., da Silva Neto, D.N., Jacques, C., Pimentel, E., Weaver, D., Lecampion, J.-F., Doncel, F., Momiyama, T., Tancredi, G., 2006. Charon's size and an upper limit on its atmosphere from a stellar occultation. Nature 439 (7072), 52–54.
Simonelli, D.P., Reynolds, R.T., 1989. The interiors of Pluto and Charon: structure, composition, and implications. Geophys. Res. Lett. 16 (11), 1209–1212.
Stern, S.A., 1989. Pluto: comments on crustal composition, evidence for global differentiation. Icarus 81 (1), 14–23.
Stern, S.A., 1991. On the number of planets in the outer Solar System: evidence of a substantial population of 1000-km bodies. Icarus 90 (2), 271–281.
Stern, S.A., 1992. The Pluto-Charon system. Annu. Rev. Astron. Astrophys. 30, 185–233.
Stern, S.A., Bagenal, F., Ennico, K., Gladstone, G.R., Grundy, W.M., McKinnon, W.B., Moore, J.M., Olkin, C.B., Spencer, J.R., Weaver, H.A., et al., 2015. The Pluto system: Initial results from its exploration by New Horizons. Science 350 (6258), aad1815.
Stern, S.A., Weaver, H.A., Steffl, A.J., Mutchler, M.J., Merline, W.J., Buie, M.W., Young, E.F., Young, L.A., Spencer, J.R., 2006. A giant impact origin for Pluto's small moons and satellite multiplicity in the Kuiper belt. Nature 439 (7079), 946–948.
Strazzulla, G., Palumbo, M.E., 1998. Evolution of icy surfaces: an experimental approach. Planet. Space Sci. 46 (9), 1339–1348.
Tholen, D.J., Buie, M.W., Grundy, W.M., Elliott, G.T., 2008. Masses of Nix and Hydra. Astron. J. 135 (3), 777.
Travis, B.J., Bland, P.A., Feldman, W.C., Sykes, M.V., 2015. Unconsolidated Ceres model has a warm convecting rocky core and a convecting mud ocean. In: Lunar and Planetary Science Conference, Vol. 46, p. 2360.
Trujillo, C.A., Jewitt, D.C., Luu, J.X., 2001. Properties of the Trans-Neptunian Belt: statistics from the Canada-France-Hawaii telescope survey. Astron. J. 122 (1), 457.
Tsiganis, K., Gomes, R., Morbidelli, A., Levison, H.F., 2005. Origin of the orbital architecture of the giant planets of the Solar System. Nature 435, 459–461.
Turcotte, D.L., Schubert, G., 1982. Geodynamics: Applications of Continuum Physics to Geological Problems. John Wiley, New York.
Volk, K., Gladman, B., 2015. Consolidating and crushing exoplanets: did it happen here? Astrophys. J. Lett. 806 (2), L26.
Walcott, R.I., 1970. Flexure of the lithosphere at Hawaii. Tectonophysics 9 (5), 435–446.
Walsh, K.J., Levison, H.F., 2015. Formation and evolution of Pluto's small satellites. Astron. J. 150 (1), 11.
Ward, W.R., Canup, R.M., 2006. Forced resonant migration of Pluto's outer satellites by Charon. Science 313 (5790), 1107–1109.
Weaver, H.A., Stern, S.A., Mutchler, M.J., Steffl, A.J., Buie, M.W., Merline, W.J., Spencer, J.R., Young, E.F., Young, L.A., 2006. Discovery of two new satellites of Pluto. Nature 439 (7079), 943–945.
Weidenschilling, S. J., 2004. Comets II. 97
Youdin, A.N., Kratter, K.M., Kenyon, S.J., 2012. Circumbinary chaos: using Pluto's newest moon to constrain the masses of Nix and Hydra. Astrophys. J. 755 (1), 17.